

## Accepted Manuscript

Title: Solvated protons in density functional theory – a few examples

Author: P. Quaino N.B. Luque G. Soldano R. Nazmutdinov E. Santos T. Roman A. Lundin A. Groß W. Schmickler



PII: S0013-4686(13)00741-X  
DOI: <http://dx.doi.org/doi:10.1016/j.electacta.2013.04.084>  
Reference: EA 20393

To appear in: *Electrochimica Acta*

Received date: 14-2-2013  
Revised date: 10-4-2013  
Accepted date: 13-4-2013

Please cite this article as: P. Quaino, N.B. Luque, G. Soldano, R. Nazmutdinov, E. Santos, T. Roman, A. Lundin, A. Groß, W. Schmickler, Solvated protons in density functional theory – a few examples, *Electrochimica Acta* (2013), <http://dx.doi.org/10.1016/j.electacta.2013.04.084>

This is a PDF file of an unedited manuscript that has been accepted for publication. As a service to our customers we are providing this early version of the manuscript. The manuscript will undergo copyediting, typesetting, and review of the resulting proof before it is published in its final form. Please note that during the production process errors may be discovered which could affect the content, and all legal disclaimers that apply to the journal pertain.

1  
2  
3  
4  
5  
6  
7  
8  
9  
10  
11  
12  
13  
14  
15  
16  
17  
18  
19  
20  
21  
22  
23  
24  
25  
26  
27  
28  
29  
30  
31  
32  
33  
34  
35  
36  
37  
38  
39  
40  
41  
42  
43  
44  
45  
46  
47  
48  
49  
50  
51  
52  
53  
54  
55  
56  
57  
58  
59  
60  
61  
62  
63  
64  
65

# Solvated protons in density functional theory – a few examples

P.Quaino<sup>a</sup>, N. B. Luque<sup>b</sup>, G. Soldano<sup>b</sup>, R. Nazmutdinov<sup>d</sup>, E. Santos<sup>b,c</sup>,  
T. Roman<sup>b\*</sup>, A. Lundin<sup>e</sup>, A. Groß<sup>b</sup>, and W. Schmickler<sup>b\*</sup>

<sup>a</sup>PRELINE, Universidad Nacional del Litoral  
Santa Fé, Argentina

<sup>b</sup>Institute of Theoretical Chemistry, Ulm University  
D-89069 Ulm, Germany

<sup>c</sup>Facultad de Matemática, Astronomía y Física,  
IFEG-CONICET

Universidad Nacional de Córdoba, Córdoba, Argentina

<sup>d</sup> Kazan National Research Technological University,  
420015 Kazan, Russian Federation

<sup>e</sup> Department of Chemical and Biological Engineering,  
Chalmers University of Technology  
SE-41296 Gothenburg, Sweden

April 10, 2013

## Abstract

We have investigated several ways of introducing a solvated proton into a DFT calculation in order to mimic an electrochemical interface: an extra hydrogen introduced into a metal bilayer, a Zundel and an Eigen ion. In all these cases the charge on the supposed proton is substantially less than a unit positive charge. In contrast, when the electrode is represented as a cluster, the charge on Zundel ion is indeed plus one. However, the distribution of the compensating charge on the cluster is quite different from that on a plane metal surface.

# 1 Introduction

During the last decade, much effort has been spent in modeling electrochemical interfaces with density functional theory (DFT). One of the principal difficulties is to incorporate charge separation between the two phases, and this implies that the solvent part of the interface must contain ions. When DFT is used in the periodic slab configuration, it is not straightforward to put ions into the system. DFT minimizes the energy of the system, and places the electrons wherever it is energetically most favorable. If there is sufficient solvent in the system, ions that are stable in water should form spontaneously, as can be seen by going through a simple Born-Haber cycle. Let us take the proton, on which this article is focused, as an example. A single hydrogen atom placed in water does not interact strongly with its surroundings. Taking an electron away costs about 13.6 eV, but the gain in solvation energy is -11.3 eV; placing the electron onto the electrode entails an energy gain given by the work function, which for metals are of the order of 4 – 5 eV. Thus the formation of the proton is favorable when the hydrogen is not adsorbed on the electrode. However, this argument holds only if the solvation of the proton in the model system is sufficiently strong. Also, this argument ignores the electric field that is formed at the interface when the electron is transferred to the metal, and which also stores energy. In real systems this field will be shielded by the reorientation of water, but in the model this can only happen if there is sufficient water.

However, an advice like: ‘use sufficient water’ is not really useful, since adding water molecules is computationally expensive. Therefore, we examine here the charge on the proton in a few common configurations: an extra hydrogen atom added to a water bilayer on Pt(111), a Zundel ion  $\text{H}_5\text{O}_2^+$  and an Eigen ion  $\text{H}_9\text{O}_4^+$  on Au and Pt surfaces, both in the absence and in the presence of an external field. Finally, we consider the situation for a Zundel ion in front of a metal cluster calculated by the Gaussian program, which does not use the slab configuration, and allows to place charges onto atoms. The technical details for the reported calculations have been relegated to the appendix.

## 2 Proton in a water bilayer on Pt(111)

In the vacuum, water adsorbs on Pt(111) at low temperatures and forms a water bilayer, whose structure is well-documented in the literature [1]. Therefore, a metal slab in contact with one or more bilayers of water has become quite a popular model for the electrochemical interface [2], and the group of Nørskov et al. [3] have charged this interface by adding extra hydrogen atoms to the bilayer, which acquired a positive charge. In order to investigate the charge

1  
2  
3  
4  
5  
6  
7  
8  
9  
10 separation in models of the electrochemical interface based on the water bi-  
11 layer, we have investigated the following situation: Hydrogen atoms adsorb  
12 strongly on platinum, and in the potential region where hydrogen evolution  
13 takes place, the Pt(111) surface is already covered by hydrogen atoms strongly  
14 adsorbed in the fcc(111) hollow sites. We have therefore considered a Pt(111)  
15 surface covered with a monolayer of this strongly adsorbed hydrogen  $H_s$  – in  
16 the electrochemical literature this hydrogen is also known as upd hydrogen,  
17 i.e. hydrogen deposited at underpotential – and by two layers of water within  
18 the familiar  $2\sqrt{3} \times 2\sqrt{3}R30^\circ$  geometry. This structure was allowed to relax  
19 at zero Kelvin. To this system we added a single hydrogen atom adsorbed  
20 on a top site, which is the next favorable site. The corresponding adsorbed  
21 hydrogen is known as weakly adsorbed hydrogen  $H_w$ , or opd hydrogen (ad-  
22 sorbed at overpotentials). This setup was used as the starting configuration  
23 in an ab initio molecular dynamics (AIMD) simulation performed at room  
24 temperature; the technical details have been published in ref. [4].  
25  
26

27 The motion of the weakly adsorbed hydrogen and the concomitant changes  
28 in charge distribution, obtained from Bader analysis, are shown in Fig. 1. At  
29 short times, a slight rearrangement of the hydrogen atoms, which are the  
30 lightest particles, takes place. The adsorbed hydrogen atoms repel each other,  
31 and the strongly adsorbed hydrogen atoms move a little away from the fcc  
32 hollow sites [5]. The average position of the  $H_w$  atom at first does not change  
33 much, till suddenly, after about 8.2 ps, it jumps into the water layer, where  
34 it becomes solvated. Obviously, this jump requires a favorable fluctuation in  
35 the water, which has to assume a configuration that is suitable to accept  
36 another hydrogen atom. Note the large fluctuations in the position of the  
37 extra hydrogen after it has jumped to the water layer. Qualitatively similar  
38 behaviour of the charge distribution of a solvated proton on a mercury surface  
39 vs. the proton-metal distance was reported previously in ref. [6] on the basis  
40 of cluster calculations  
41  
42  
43

44 For our purpose, the development of the charge on the extra  $H_w$  atom is of  
45 particular interest. In the initial state, its positive charge is quite small, of the  
46 order of 0.1 units. After it has jumped to the water layer, its charge becomes  
47 more positive, of the order of 0.6 units; evaluation of charge differences gives  
48 a somewhat smaller value of about 0.4 units. Actually, the charge on an atom  
49 is not an observable and depends on the attribution of the electronic den-  
50 sity to individual atoms. Therefore, different methods tend to give somewhat  
51 different values. The important point is that the excess charge is somewhere  
52 intermediate between zero and unity. The hydrogen atoms pertaining to water  
53 molecules also carry a positive charge of about the same magnitude, indicating  
54 that all hydrogen atoms within the layer are equivalent, like one would expect  
55 to happen in the long run. When the excess hydrogen jumps into the water  
56 layer the total charge in that layer, which now includes the extra hydrogen,  
57 also rises. The increase in the total charge of the water layer is somewhat  
58  
59  
60  
61  
62  
63  
64  
65

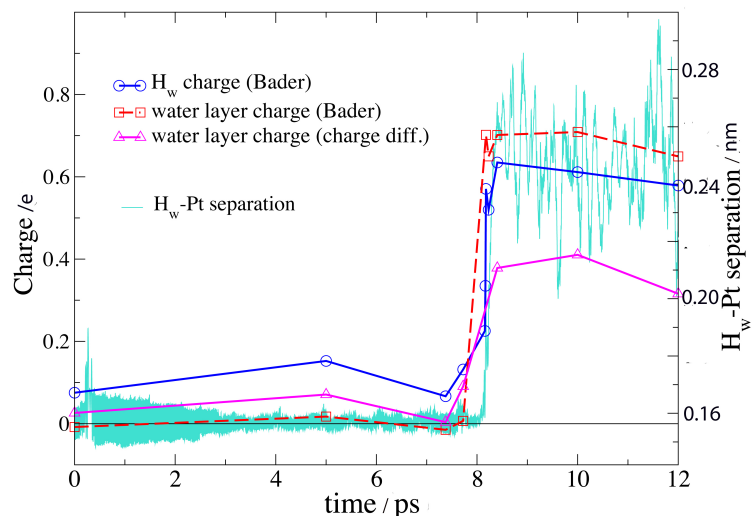


Figure 1: Position and positive charge on the extra hydrogen atom  $H_w$  and charge on the water layer over the course of the molecular dynamics run.

larger than that on the extra hydrogen, indicating a certain delocalization of the positive charge. The excess positive charge within the water layer must be balanced by a negative excess charge concentrated on the metal surface. In order to investigate in detail the charge distribution we have calculated the electron density differences for  $t > 8.2$  ps, i.e. after the jump, according to:  $\Delta\rho(\mathbf{r}) = \rho_{\text{full}}(\mathbf{r}) - [\rho_{\text{Pt}+\text{H}_s}(\mathbf{r}) + \rho_{\text{H}_s\text{w}+\text{H}_2\text{O}_b}(\mathbf{r})]$ , where  $\rho_{\text{Pt}+\text{H}_s}(\mathbf{r})$  is the electron density distribution of the H-covered Pt surface, and  $\rho_{\text{H}_s\text{w}+\text{H}_2\text{O}_b}(\mathbf{r})$  is the electron density distribution of the water bilayers with the extra hydrogen. Figure 2 shows the situation after 10 ps. It clearly shows an excess negative charge located mainly on the  $\text{H}_s$  atoms, between the metal surface and the water layer, which in a classical context would be an image charge, i.e. the surface charge which mimics an image inside the metal.

### 3 Zundel and Eigen ion

In water at ambient temperatures, there are two stable forms of the solvated proton: the Zundel ion  $\text{H}_5\text{O}_2^+$  and the Eigen ion  $\text{H}_9\text{O}_4^+$ . In the vacuum the Zundel ion has almost  $\text{C}_{2v}$  geometry, when it is adsorbed on a metal surface it lies flat. The energy of ionization of the neutral molecule  $\text{H}_5\text{O}_2$  is about 4.36 eV. Therefore, at a first glance one should expect a transfer of an electron to metals with work functions larger than this value. However, this simple consideration disregards the fact, that DFT can place partial charges onto

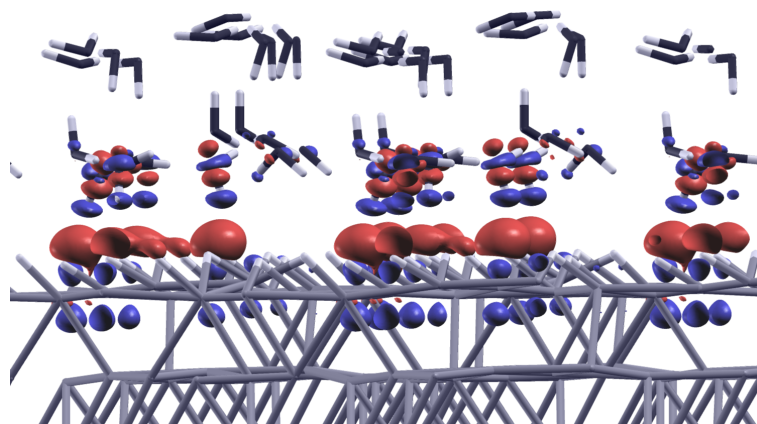


Figure 2: Distribution of the excess charge after 10 ps. Red indicates electron buildup.

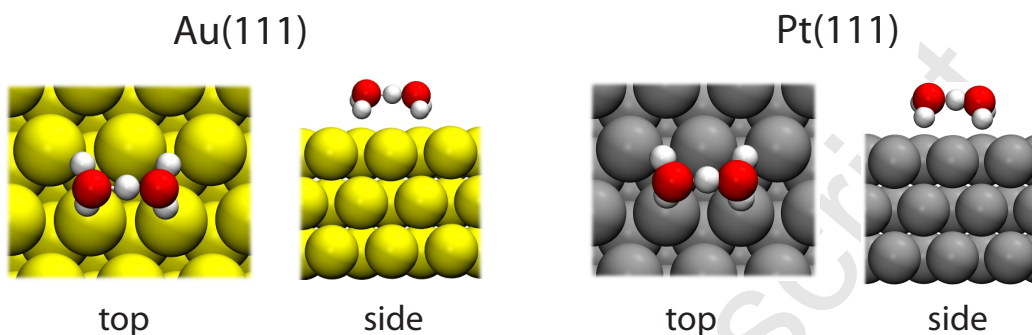
atoms even if they do not participate in a chemical bond; in addition, as mentioned before, an ion in front of a metal surfaces generates an electric field, which also contains energy.

We have studied the adsorption of the Zundel molecule  $\text{H}_5\text{O}_2$  on several surfaces – by calling it a molecule we anticipate that it carries little excess charge. Typical configurations for the adsorption on (111) surfaces are shown in Fig. 3. The corresponding energies of adsorption are given in Tab. 1. Considering the fact that water adsorbs but weakly on metal surfaces, the adsorption energies for the Zundel species are surprisingly large, indicating a chemical bond formation. They are of the same order of magnitude as the adsorption energies for a single hydrogen atom. Adsorption on the more open Au(100) surface is notably stronger than on the others. For Pt(111) and Ag(111) we have varied the surface coverage by changing the size of the unit cell. The adsorption energies becomes substantially less negative with coverage, which shows that the adsorbates repel each other; we will return to this point below.

Au(100)	Au111	Pt(111)		Ag(111)	
$3 \times 3$	$3 \times 3$	$3 \times 3$	$4 \times 4$	$3 \times 3$	$4 \times 4$
-3.52	-2.29	-3.04	-3.49	-1.97	-2.29

Table 1: Adsorption energies of the Zundel molecule on various substrates and for various sizes of the unit cell; all energies are in eV.

In this article we are especially interested in the charge distribution to



22 Figure 3: Top and side views of the Zundel molecule adsorbed on Au(111) and  
23 Pt(111).  
24

25  
26  
27 see, to what extent the adsorbate is positively charged. For this purpose we  
28 have calculated the integrated charge difference as a function of the distance  
29 perpendicular to the metal surface (see. Fig. 4). For comparison, we also show  
30 the distribution for the case in which the central hydrogen atom has been  
31 eliminated, keeping the other atoms fixed. Both on Au(111) and on Pt(111)  
32 the Zundel molecule does carry a positive excess charge, which is compensated  
33 by a negative charge located mainly between the Zundel molecule and the  
34 metal surface. When the central hydrogen atom has been eliminated, a positive  
35 charge remains, but it is substantially smaller. Note that this positive charge  
36 is larger in the case of Pt(111), indicating a stronger interaction. Mulliken  
37 analysis gives an excess charge of the order of 0.1 units in all investigated  
38 cases, which is somewhat smaller than the excess charge distribution shown  
39 in the figure, which is about 0.24 - 0.25. The excess charge on the adsorbed  
40 species is probably the cause for the repulsion that we observed above. Thus,  
41 the two water molecules attached to the central hydrogen atom do not provide  
42 enough solvation energy to induce a sizable ionization.  
43  
44  
45  
46

47 The Eigen ion (see Fig. 5) has twice as many water molecules; however,  
48 the ionization energy of the neutral species is 4.18 eV and thus not much  
49 higher than that of the Zundel molecule. We have investigated two adsorption  
50 structures with high symmetry on a Au(100), which are shown in the figure.  
51 The structure on the right of the figure has two water molecules pointing  
52 towards the surface, and the third is directed towards the vacuum; it has an  
53 adsorption energy of -3.19 eV and is locally stable. The one in the center  
54 has three of its four water molecules in contact with the surface, and has a  
55 larger energy of adsorption, -3.73 eV, and is the most stable configuration. The  
56 former has a positive Mulliken charge of 0.4, the latter of only 0.23; neither  
57 structure shows spin polarization.  
58  
59  
60  
61  
62  
63  
64  
65

1  
2  
3  
4  
5  
6  
7  
8  
9  
10 The overall charge distribution is similar to that for the Zundel ion, show-  
11 ing a positive charge on the Eigen molecule compensated by a negative charge  
12 on the metal surface. However, the charge separation is appreciably larger.  
13 Thus, the larger number of water molecules in the Eigen species induces a  
14 larger charge localization than for the Zundel molecule, but less than for the  
15 extra hydrogen atom in the bilayer structure.

16 The positive charge on the ions can be increased by applying a field which  
17 raises the electronic levels; this is equivalent to placing a negative excess charge  
18 on the metal. In the case of the two structures investigated for the eigen ion,  
19 the most favorable structure (center in Fig. 5) requires a field of the order of 2  
20  $\text{V}\text{\AA}^{-1}$  to achieve unit positive charge. The other structure, which has a higher  
21 excess charge to start with, requires a lower field of about  $1.3 \text{V}\text{\AA}^{-1}$ . These  
22 fields are somewhat higher than those encountered in electric double layers,  
23 which are typically of the order of a few tenths of  $\text{V}\text{\AA}^{-1}$ . We note that placing  
24 a positive charge onto a molecule by application of a field is less problematic  
25 than placing a negative charge. When the corresponding positive field is high,  
26 at large distances the vacuum level drops below the Fermi level, and may  
27 accumulate negative charge, which is unphysical [7]. This can be prevented by  
28 using a code with localized orbitals, which has no states in the distant vacuum  
29 region. For details we refer to calculations with  $\text{OH}^-$  and  $\text{O}_2^-$  [8,9].

30 Charge localization is much easier to achieve for protons above a small  
31 cluster of metal atoms using a program like Gaussian. As an example, we  
32 discuss results for a Zundel ion above a two layer  $\text{Au}_{15}(10+5)$  cluster repre-  
33 senting a  $\text{Au}(111)$  surface. In Gaussian, one can specify the total charge  $Q$  on  
34 the system, and we have investigated both for a positive unit charge  $Q = 1$ ,  
35 and for  $Q = 0$ . For  $Q = 1$  the Mulliken charge on the Zundel ion is 0.7, while  
36 the Natural Population Analysis (NPA) gives 1, For  $Q = 0$  the correspond-  
37 ing values are 0.65 (Mulliken) and 0.98 (NPA). Thus the Zundel ion acquires  
38 automatically a positive charge of about +1, which is an advantage of such  
39 cluster calculations. However, the counter charge tends to be accumulated at  
40 the edges of the cluster for electrostatic reasons; therefore it depends on the  
41 size of the cluster, and is far from the image-like distribution one would ex-  
42 pect on a plane surface. The ionization energy of the cluster is 6.3 eV, and the  
43 affinity 3.1 eV. For comparison, the work function of  $\text{Au}(111)$  obtained from  
44 our cluster calculations is 5.22 eV. Thus, the electron affinity of the cluster  
45 cannot be the reason for the larger charge separation in the cluster calcula-  
46 tion. It is rather the distribution of the extra charge, which is more favorable  
47 at the edges of a cluster than on a planar surface.  
48  
49  
50  
51  
52  
53  
54  
55  
56  
57  
58  
59  
60  
61  
62  
63  
64  
65



## 4 Conclusions

We have investigated three different structures meant to represent a proton: an extra hydrogen atom within a water bilayer, a Zundel and an Eigen ion. The slab configuration does not result in a unit positive excess charge in any of these cases. This remains true even if we account for the uncertainty in the evaluation of an excess charge: Mulliken and Bader analysis always give somewhat different values, and this is true of the various alternatives. We encountered the highest positive charge for the extra hydrogen in the bilayer, a somewhat lower charge in the Eigen ion, while the Zundel ion is almost uncharged. Thus, charge localization increases with the amount of water, which was to be expected. In any case, when attempting to model the electric double layer one has to consider the fact that in all the cases investigated the proton carries at best a partial positive charge.

Cluster calculation with Gaussian do not have any difficulties to localize a complete positive charge on the proton, and may therefore be an attractive alternative for some purposes. The disadvantages are the finite size of the cluster and the artificial distribution of the counter charge on the metal.

## Acknowledgements

Financial support by the Deutsche Forschungsgemeinschaft (Schm 344/34-1,2, SCHM 344/42-1,2, Sa 1770/1-1,2, and FOR 1376), by RFBR (11-03-01186-a), and by CONICET (PIP 112- 201001-00411), and by the international cooperation between CONICET and DFG, are gratefully acknowledged. We thank CONICET, Argentina, for continued support. A generous grant of computing time from the Baden- Württemberg grid is gratefully acknowledged.

## A Technical Details

### A.1 AIMD simulations

The total energy calculations for the proton in the water bilayer total-energy calculations were carried out using the periodic DFT package VASP [10], employing the generalized gradient approximation (GGA) to describe the exchange-correlation effects by employing the exchange-correlation functional by Perdew, Burke and Ernzerhof (PBE) [11]. The ionic cores were represented by projector augmented wave (PAW) potentials [12] as constructed by Kresse and Joubert [13]. The electronic one-particle wave function were expanded in a plane-wave basis set up to an energy cutoff of 400 eV. The Pt(111) substrate was represented by a four-layer slab, of which the outermost two layers were always given full degrees of freedom to move during the geometry optimization

1  
2  
3  
4  
5  
6  
7  
8  
9 and in the molecular dynamics runs as well.

10 Ab initio molecular dynamics (AIMD) simulations were performed using  
11 the Verlet algorithm [14] at a temperature of 300 K within the microcanoni-  
12 cal ensemble for at least 11 ps. As a rule of the thumb, the time step in MD  
13 simulations should be approximately one-tenth of the shortest period of mo-  
14 tion [15]. As far as water is concerned, this corresponds to the O-H stretch  
15 vibrational period which is typically about 10 fs. Hence we have chosen a time  
16 step of 1 fs.  
17

18 The Pt(111)-water interface was modeled with two water layers within a  
19  $2\sqrt{3} \times 2\sqrt{3}R30^\circ$  geometry, leading to 12 metal atoms and 8 water molecules  
20 per layer. Energy-minimum structures of the water bilayers were used as the  
21 initial configurations of the molecular dynamics runs, and were determined  
22 using  $4 \times 4 \times 1$   $k$  points until the energies were converged to within  $10^{-4}$  eV.  
23 For the molecular dynamics simulations, the energy cutoff was reduced to 350  
24 eV and  $2 \times 2 \times 1$   $k$  points were used to obtain a compromise between sufficient  
25 accuracy and manageable simulation time. Water layers on Pt(111) in an  
26 ultra-high vacuum chamber typically desorb at temperatures above 200 K [16,  
27 17]. Consequently, in order to prohibit the water layers from desorbing in our  
28 computational setup, the height of two oxygen atoms per surface unit cell in  
29 the second water layer above the surface (but not their lateral position) was  
30 fixed. This means that just two out of 144 spatial degrees of freedom of the  
31 water layer are not treated dynamically.  
32

33 It should be noted that for a single water bilayer on Pt(111) it has been  
34 shown that the combination of so-called flat-lying and H-down oriented water  
35 molecules comprise the stable structure [18] if a  $\sqrt{3} \times \sqrt{3}R30^\circ$  periodicity is  
36 assumed. The presence of the second bilayer, however, influences the structure  
37 of the first water layer. It stabilizes the H-up orientation for the molecules of  
38 the first hexagonal bilayer, as the stronger hydrogen bonding between the  
39 water molecules in this configuration lowers the total energy. The presence  
40 of surrounding water weakens an individual water molecule's bond with the  
41 metal surface, of which one consequence is a substantial shift of the position  
42 of water from the platinum surface, from 2.4 Å for a single water molecule on  
43 platinum to about 3.2 Å for the ordered water bilayers in. In order to maximize  
44 the hydrogen bonding in the double-bilayer structure, the two honeycomb  
45 lattices of water are stacked directly against each other, but with the water  
46 molecules staggered in terms of their relative orientations: H-down-oriented  
47 molecules lie right above the flat-lying molecules of the first bilayer, while  
48 flat-lying molecules are positioned right above the H-up molecules of the first  
49 bilayer.  
50  
51  
52  
53  
54  
55  
56  
57  
58  
59  
60  
61  
62  
63  
64  
65

## A.2 Zundel and Eigen ions

The calculations for the Zundel and Eigen ions were performed both with the SIESTA [19] and the DACAPO codes [21]; when both codes were used, they gave practically the same results. We used the generalized gradient approximation in the version of Perdew *et al* [11] with spin polarization. The ion cores were described by non-conserving non-relativistic pseudopotentials [20] and a double- $\zeta$  plus polarization basis of localized orbitals were used to expand the wavefunctions in the SIESTA code. All calculations were performed with an energy mesh cut-off of 300 Ry and a k-point mesh of  $4 \times 4 \times 1$  in the Monkhorst-Pack scheme [4]. The energy accuracy was reached when the change in the absolute energy value was less than 10 meV, and for geometry optimization the convergence criterion was achieved when the force on each atom was less than  $0.02 \text{ eV/\AA}$ . In all the calculations 12 layers of vacuum were considered. Unless mentioned, the metal layers were fixed at the calculated nearest-neighbor distance corresponding to bulk. To evaluate the adsorption of the eigen molecule on Au(100), two possibilities for the initial position of the molecule were considered (see Fig. 5). In the configurations, the molecule was completely free to relax in the xyz the coordinates.

## A.3 Calculations with Gaussian

The DFT calculations were performed using the M062X functional as implemented in the Gaussian 09 program suit [22]. A basis set of DZ quality was employed to describe the valence electrons of the Au atoms, while the effect of inner electrons was addressed by the Effective Core Potential developed by Hay and Wadt (LanL2). The standard basis set 6-31g(d, p) was used for the electrons of O and H atoms. The Au(100) electrode surface was described using a two-layer clusters of Au<sub>14</sub>(8+6). The open shell systems were treated in terms of the unrestricted formalism. The geometry of the adsorbates was optimized without symmetry restrictions.

## References

- [1] see e.g. A. Michaelides, Density functional theory simulations of water-metal interfaces: waltzing waters, a novel 2D ice phase, and more, *Appl. Phys. A*, 85 (2006) 415.
- [2] J. Rossmeisl, E. Skulason, M. E. Björketun, V. Tripkovic, J. K. Nørskov, Modeling the electrified solidliquid interface, *Chem. Phys. Lett.* 466 (2008) 68.
- [3] E. Skulason, G. S. Karlberg, J. Rossmeisl, T. Bligaard, J. Greeley, H. Jonsson, and Jens K. Nørskov, Density functional theory calculations for

- 1  
2  
3  
4  
5  
6  
7  
8  
9 the hydrogen evolution reaction in an electrochemical double layer on the  
10 Pt(111) electrode, *Phys. Chem. Chem. Phys.* 9 (2007) 3241.  
11  
12 [4] T. Roman and A. Groß, Structure of water layers on hydrogen-covered  
13 Pt electrodes, *Catalysis Today*, 202, (2013), 183.  
14  
15 [5] E. Santos, P. Hindelang, P. Quaino, E. N. Schulz, G. Soldano and W.  
16 Schmickler, Hydrogen Electrocatalysis on Single Crystals and on Nano-  
17 structured Electrodes, *ChemPhysChem* 12 (2011) 2274.  
18  
19 [6] R.R. Nazmutdinov, M.D. Bronshtein, F. Wilhelm, A.M. Kuznetsov,  
20 Challenge of the discharge of a hydronium ion at a mercury electrode:  
21 Beyond the Tafel plots, *J. Electroanal. Chem.* 607 (2007) 175-183.  
22  
23 [7] S. Schnur and A. Groß, Challenges in the first-principles description of  
24 reactions in electrocatalysis, *Catalysis Today*, 165 (2011) 129.  
25  
26 [8] E. Santos, P. Quaino, and W. Schmickler, Theory of electrocatalysis:  
27 hydrogen evolution and more, *Phys.Chem.Chem.Phys* 14 (2012) 11224.  
28  
29 [9] P. Quaino, N. B. Luque, R. Nazmutdinov, E. Santos, and W. Schmickler,  
30 Why is gold such a good catalyst for oxygen reduction in alkaline media?,  
31 *Angew. Chem. Int. Ed.* 51 (2012) 12997.  
32  
33 [10] G. Kresse and J. Furthmüller, Efficient iterative schemes for ab initio  
34 total-energy calculations using a plane-wave basis set, *Phys. Rev. B* 54  
35 (1996) 11169.  
36  
37 [11] J. P. Perdew, K. Burke, and M. Ernzerhof, Generalized Gradient Ap-  
38 proximation Made Simple, *Phys. Rev. Lett.* 77 (1996) 3865.  
39  
40 [12] P. E. Blöchl, Projector augmented-wave method, *Phys. Rev. B* 50 (1994)  
41 17953.  
42  
43 [13] G. Kresse and D. Joubert, From ultrasoft pseudopotentials to the pro-  
44 jector augmented-wave method, *Phys. Rev. B* 59 (1999) 1758.  
45  
46 [14] L. Verlet, Experiments” on Classical Fluids. I. Thermodynamical Prop-  
47 erties of Lennard-Jones Molecules, *Phys. Rev.* 159 (1967) 98.  
48  
49 [15] A. R. Leach, *Molecular Modelling: Principles and Applications*, Pearson,  
50 Harlow, 2nd edition, 2001.  
51  
52 [16] E. Langenbach, A. Spitzer, and H. Lüth, The adsorption of water on  
53 Pt(111) studied by irreflection and UV-photoemission spectroscopy, *Surf.*  
54 *Sci.* 147 (1984) 179.  
55  
56 [17] M. Kiskinova, G. Pirug, and H. Bonzel, Adsorption and decomposition  
57 of H<sub>2</sub>O on a K-covered Pt(111) surface, *Surf. Sci.* 150 (1985) 319.  
58  
59 [18] S. Schnur and A. Groß, Properties of metal-water interfaces studied from  
60 first principles, *New J. Phys.* 11 (2009) 125003.  
61  
62  
63  
64  
65

- 1  
2  
3  
4  
5  
6  
7  
8  
9 [19] J. M. Soler, E. Artacho, J. D. Gale, A. Garsia, J. Junquera, P. Orejon,  
10 D. Sanchez-Portal, The SIESTA method for ab initio order-N materials  
11 simulation, *J. Phys.:Condens. Matter* 14 (2002) 2745.  
12  
13 [20] O. N. Troullier, J. L. Martins, Efficient pseudopotentials for plane-wave  
14 calculations, *Phys. Rev. B*, 43 (1991) 1993  
15  
16 [21] B. Hammer, L.B. Hansen and J.K. Nørskov, Improved adsorption ener-  
17 getics within density-functional theory using revised Perdew-Burke-  
18 Ernzerhof functionals, *Phys. Rev. B* 59 (1999) 7413.  
19  
20 [22] Gaussian 09, Revision A.1, Frisch, M. J.; Trucks, G. W.; Schlegel, H. B.;  
21 Scuseria, G. E.; Robb, M. A.; Cheeseman, J. R.; Scalmani, G.; Barone,  
22 V.; Mennucci, B.; Petersson, G. A.; Nakatsuji, H.; Caricato, M.; Li, X.;  
23 Hratchian, H. P.; Izmaylov, A. F.; Bloino, J.; Zheng, G.; Sonnenberg, J.  
24 L.; Hada, M.; Ehara, M.; Toyota, K.; Fukuda, R.; Hasegawa, J.; Ishida,  
25 M.; Nakajima, T.; Honda, Y.; Kitao, O.; Nakai, H.; Vreven, T.; Mont-  
26 gomery, Jr., J. A.; Peralta, J. E.; Ogliaro, F.; Bearpark, M.; Heyd, J. J.;  
27 Brothers, E.; Kudin, K. N.; Staroverov, V. N.; Kobayashi, R.; Normand,  
28 J.; Raghavachari, K.; Rendell, A.; Burant, J. C.; Iyengar, S. S.; Tomasi,  
29 J.; Cossi, M.; Rega, N.; Millam, J. M.; Klene, M.; Knox, J. E.; Cross, J.  
30 B.; Bakken, V.; Adamo, C.; Jaramillo, J.; Gomperts, R.; Stratmann, R.  
31 E.; Yazyev, O.; Austin, A. J.; Cammi, R.; Pomelli, C.; Ochterski, J. W.;  
32 Martin, R. L.; Morokuma, K.; Zakrzewski, V. G.; Voth, G. A.; Salvador,  
33 P.; Dannenberg, J. J.; Dapprich, S.; Daniels, A. D.; Farkas, Ö.; Foresman,  
34 J. B.; Ortiz, J. V.; Cioslowski, J.; Fox, D. J. Gaussian, Inc., Wallingford  
35 CT, 2009.  
36  
37  
38  
39  
40  
41  
42  
43  
44  
45  
46  
47  
48  
49  
50  
51  
52  
53  
54  
55  
56  
57  
58  
59  
60  
61  
62  
63  
64  
65

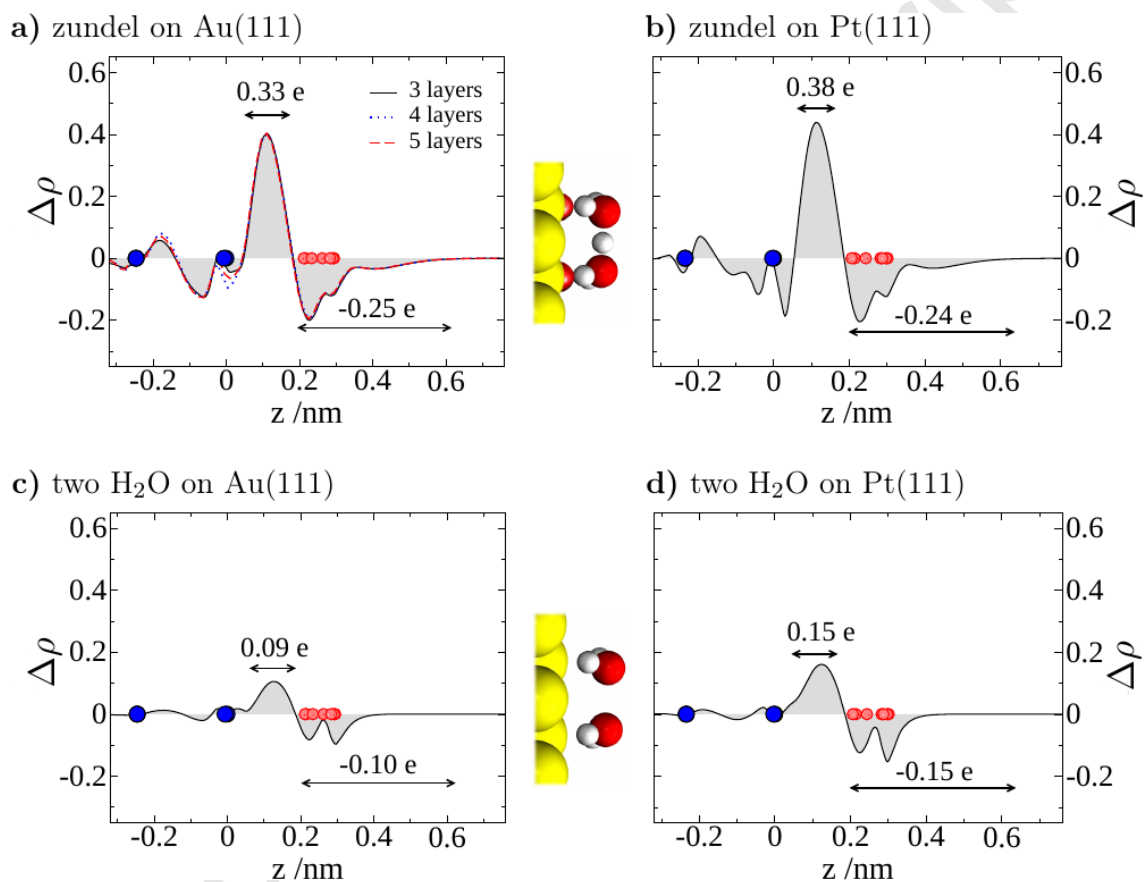


Figure 4: Distribution of the integrated excess charge  $\Delta\rho$  along the  $z$  axis perpendicular to the metal surface for Au(111) and Pt(111). The upper panels show the case for the adsorbed Zundel molecule; the lower panels illustrates the case in which the central hydrogen atom of the Zundel molecule has been eliminated. Positive values correspond to electron accumulation, negative values to depletion. The blue circles indicate metal surface atoms, the red circles the atoms of the Zundel molecule.

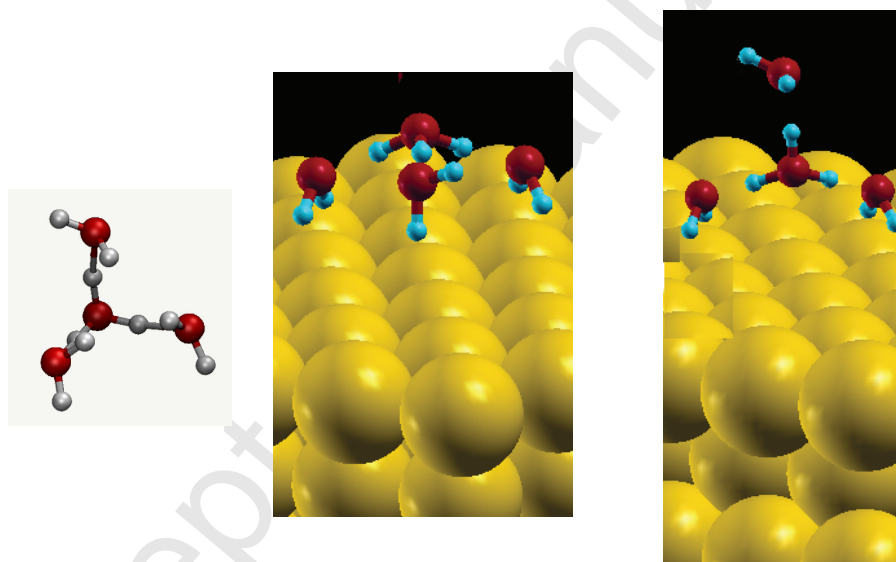


Figure 5: Structure of an Eigen ion in vacuum (left) and two adsorption structures for the Eigenion on Au(100) with high symmetry; the structure in the middle is the most favorable.